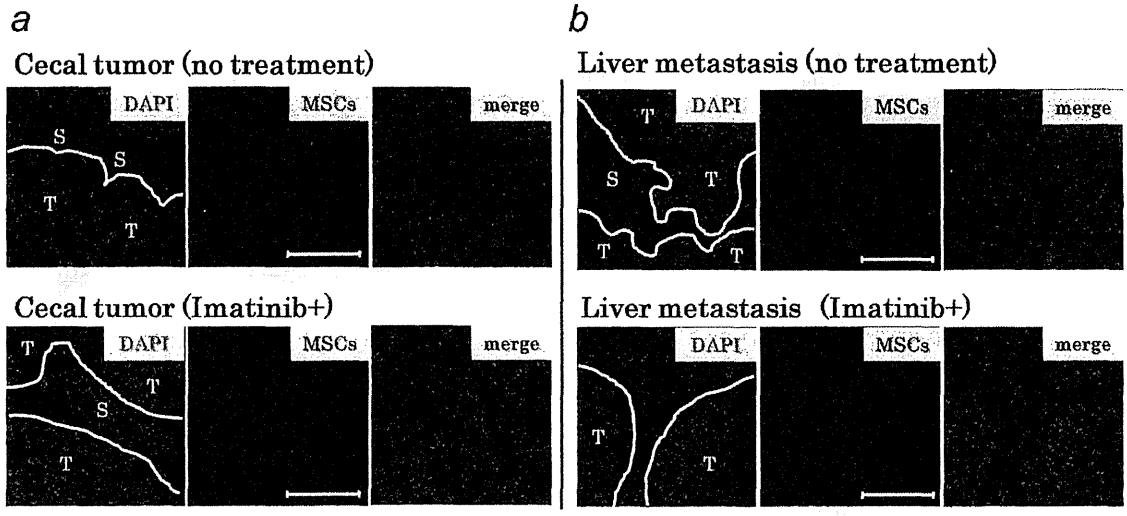

Figure 2. Migration of MSCs to orthotopic colon tumors and metastatic liver tumors. Systemically administered and PKH26-labeled MSCs (red) migrated to (*a*) the stroma of orthotopic colon tumors and (*b*) metastatic liver tumors. Imatinib treatment inhibited tumor-homing ability of MSCs *in vivo*. 4′,6-diamidino-2-phenylindole (DAPI) staining for cell nuclei (blue) shows outline of the stroma within tumor tissue. T: tumor nest, S: stroma, scale bars: 100 μm.

μm pore size, Corning Costar). After 24 hr, upper chambers containing KM12SM cells were set into the lower chambers in serum-free culture medium with or without 1 μM imatinib. After 1 hr of incubation at 37°C, inserts were removed. After 3 washes with cold phosphate-buffered saline containing 1 mmol/L sodium orthovanadate, MSCs were lysed. Unstimulated KM12SM cells were also lysed. Proteins (total protein 20 μg) were separated by SDS-PAGE and transferred to nitrocellulose transfer membranes (Whatman GmbH, Dassel, Germany). The immune complexes were visualized by enhanced chemiluminescence with an ECL Plus Kit (GE Healthcare, Buckinghamshire, UK).

Semiquantitative reverse transcription-polymerase chain reaction (RT-PCR)

Total RNA was extracted from gastric carcinoma cell lines with an RNeasy Kit (Qiagen, Tokyo, Japan) according to the manufacturer's instructions. RT-PCR was performed with the isolated RNA (1 μg). cDNA was generated from 1 μg of total RNA with a first-strand cDNA synthesis kit (Amersham Biosciences, Buckinghamshire, UK). Semiquantitative RT-PCR was performed with an AmpliTag Gold Kit (Roche, Mannheim, Germany) according to the manufacturer's instructions. RT-PCR reactions without reverse transcription showed no specific bands. Respective primer sequences, annealing temperatures, and PCR cycles were as follows: PDGFR-β forward, AGC TACCCCTCAAGGAATCATAG and PDGFR-β reverse, CTC TGGTGGATGGATTAAGACTG (PDGFR-β PCR product, 376 bp; 58°C; 30 cycles); and GAPDH forward, ATCATCCCT GCCTCTACTGG and GAPDH reverse, CCCTCCGACGC CTGCTTCAC (GAPDH PCR product, 188 bp; 58°C; 28 cycles); and PDGF-B forward, CGAGTTGGACCTGAAC ATGA and PDGF-B reverse, GTCACCGTGGCCTTCTTAAA (PDGF-B PCR product, 339 bp; 58°C; 30 cycles).

Statistical analysis

Values are expressed as mean ± standard error (SE). Survival curves were drawn by the Kaplan and Meier method, and the log rank test was used to analyze differences in survival rates. Student's- or Welch's *t*-test or the Wilcoxon test was used to analyze differences in other variables, as appropriate. Probability values of <0.05 were considered significant. All statistical analyses were performed with JMP software (SAS Institute, Cary, NC).

Results

Effect of imatinib on interaction between KM12SM cells and MSCs in vitro

RT-PCR and Western blotting revealed that MSCs expressed PDGFR-β and KM12SM cells expressed PDGF-B in culture conditions (Figs. 1*a* and 1*b*). PDGFR-β was expressed by MSCs but not by KM12SM cells, and phosphorylation of PDGFR-β in MSCs was completely inhibited by 1 μM imatinib (Fig. 1*b*). When the effects of imatinib on migration of MSCs were examined by migration assay, we found more MSCs migrated toward tumor cell culture than toward the medium without tumor cells; however, this effect was impaired with imatinib treatment (24.9 ± 2.5 *vs.* 43.4 ± 3.0 cells/field, $p < 0.05$; 9.3 ± 1.1 *vs.* 10.7 ± 1.1 cells/field) (Fig. 1*c*). We performed cell proliferation assay and confirmed that 1 μM imatinib did not affect cell proliferation of MSCs at least for 3 days (Fig. 1*d*).

To examine the effect of imatinib on the growth of KM12SM cells *in vitro*, cell proliferation assay was performed.

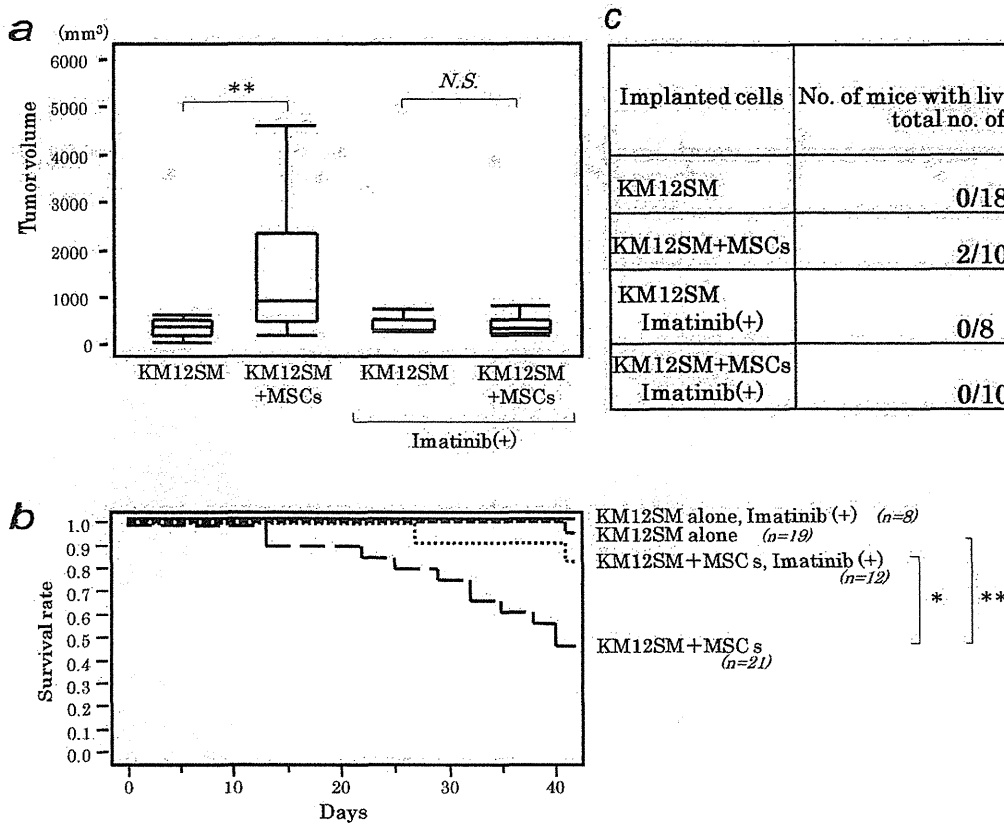

c

Implanted cells	No. of mice with liver metastasis/ total no. of mice
KM12SM	0/18
KM12SM+MSCs	2/10
KM12SM Imatinib(+)	0/8
KM12SM+MSCs Imatinib(+)	0/10

Figure 3. Comparisons of outcomes (cecal coinjection studies). Mice were divided into four groups according to the kind(s) of implanted cells and the treatment received, and mice surviving to day 42 were necropsied: (*i*) KM12SM cells alone without imatinib treatment (n = 18), (*ii*) KM12SM cells mixed with MSCs without imatinib treatment (n = 10), (*iii*) KM12SM cells alone with imatinib treatment (n = 8), or (*iv*) KM12SM cells mixed with MSCs with imatinib treatment (n = 10). (*a*) Transplantation of KM12SM cells mixed with MSCs (0.5×10^6:1.0×10^6, n = 10) resulted in significantly greater tumor volume than that resulting from transplantation of KM12SM cells alone (0.5×10^6, n = 18). Imatinib treatment impairs tumor promoting effect of MSCs (KM12SM cells alone, n = 8 mice; KM12SM cells with MSCs, n = 10 mice). $^{**}p < 0.01$, bars: SE. (*b*) Kaplan-Meier curves showing survival of mice bearing KM12SM cells alone (with or without imatinib treatment n = 8 or n = 19) and KM12SM cells mixed with MSCs (with or without imatinib treatment; n = 12 or n = 21). The survival rate was significantly lower in the mixed-cell group, and imatinib treatment significantly improved the survival rate in the mixed-cell group. $^{*}p < 0.05$, $^{**}p < 0.01$ (by log rank test). (*c*) Surviving mice were necropsied on day 42. The number of mice with liver metastasis is indicated. Macroscopic liver metastasis was seen only in the mixed-cell group that did not receive imatinib treatment.

The reported clinically effective plasma concentration of imatinib is 1 to 5 μM. The proliferation of KM12SM cells was not affected by imatinib treatment when the concentration of imatinib was increased up to 8 μM (Fig. 1*e*).

Imatinib inhibited MSC migration to orthotopic colon tumors and metastatic liver tumors

After injection of PKH-labeled MSCs into the tail veins of tumor-bearing mice, MSCs were detected specifically in the tumor stroma both at the primary site (colon) and the metastatic site (liver). In the imatinib treatment groups, no MSCs were detected in tumor stroma (Figs. 2*a* and 2*b*).

Imatinib inhibited tumor-promoting effect of MSCs in the orthotopic colon tumor model

The volumes of tumors resulting from transplantation of mixed cells was significantly greater than the volumes of tumors resulting from transplantation of tumor cells alone (511 ± 127 mm^3 *vs.* 1,478 ± 467 mm^3, $p < 0.01$). In the imatinib treatment groups, the tumor-promoting effect of MSCs was impaired (417 ± 61 mm^3 *vs.* 408 ± 67 mm^3) (Fig. 3*a*). The survival of mice was significantly lower in the mixed-cell group than in the group that received KM12SM cells alone ($p < 0.01$), and survival in the mixed-cell group that received imatinib was significantly improved ($p < 0.05$) (Fig. 3*b*). Macroscopic liver metastases were seen only in the mixed-cell group that did not receive imatinib (Fig. 3*c*). To clarify the mechanisms underlying the inhibitory effect of imatinib, we examined proliferation (PCNA-LI), apoptosis (AI), and angiogenesis (MVA) in primary tumors by immunohistochemistry. Between groups not given imatinib treatment, the PCNA-LI was significantly higher in the mixed-cell group than in the tumor-cell-alone group (30.6 ± 4.7 *vs.* 62.8 ± 4.6%, $p < 0.01$) (Fig. 4*a*), the AI was significantly lower in the mixed-cell group (7.2 ±

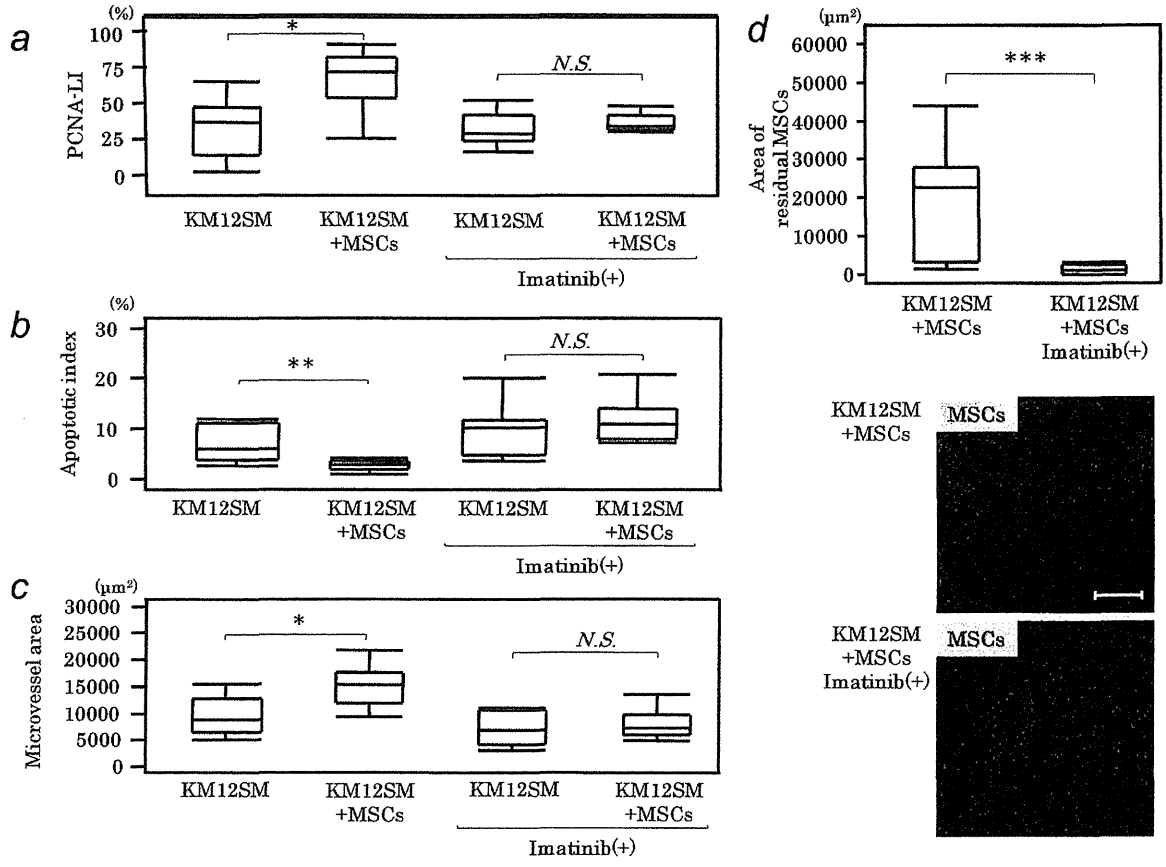

Figure 4. Proliferation, apoptosis, and angiogenesis in the four groups classified according to the kind(s) of implanted cells and the treatment received. (*a*) Proliferating cell nuclear antigen labeling index (PCNA-LI), (*b*) apoptotic index, and (*c*) microvessel area were analyzed by immunohistochemistry of the orthotopic colon tumors. Tumors from the mixed-cell group had a significantly higher PCNA-LI, a significantly lower AI, and significantly greater MVA than tumors from the group that received KM12SM cells alone. Imatinib treatment impaired the effects of MSCs.*$p < 0.05$, bars: SE; **$p < 0.01$, bars: SE. (*d*) Surviving MSCs in the tumor microenvironment *in vivo*. Three weeks after cecal transplantation of KM12SM cells mixed with PKH26-labeled MSCs, surviving MSCs were significantly fewer in the imatinib treatment group than in the control group. Lower panels are representative photomicrographs of stained sections. ***$p < 0.001$, bars: SE. Scale bars: 100 μm.

1.1 *vs.* 2.8 ± 0.3%, $p < 0.01$) (Fig. 4*b*), and the MVA was significantly greater in the mixed-cell group (9,715 ± 1,156 *vs.* 15,180 ± 1,225 μm^2, $p < 0.05$) (Fig. 4*c*). With imatinib treatment, there was no significant difference between mice injected with tumor cells alone and those injected with mixed cells in PCNA-LI (33.4 ± 2.8 *vs.* 39.4 ± 2.2%), in AI (9.5 ± 1.6 *vs.* 11.8 ± 1.3%), or in MVA (7,227 ± 967 *vs.*7919 ± 835 μm^2) (Figs. 4*a*–4*c*).

Survival of MSCs decreased with imatinib treatment in vivo

Three weeks after transplantation of KM12SM cells mixed with PKH26-labeled MSCs, the PKH26-positive areas were significantly smaller in the imatinib treatment group than in the group not treated with imatinib (19,830 ± 4,485 *vs.* 2,005 ± 868 μm^2, $p < 0.001$) (Fig. 4*d*).

PDGFR-β in MSCs was phosphorylated, which was inhibited by imatinib treatment

We found that PDGFR-β in MSCs was phosphorylated 3 weeks after transplantation of KM12SM cells mixed with PKH26-labeled MSCs, and it was inhibited by imatinib treatment (Fig. 5).

Imatinib inhibited the tumor-promoting effect of MSCs in the liver metastasis model

Transplantation of KM12SM cells alone into the spleen of nude mice resulted in formation of liver metastases in 70% of the animals, and the rate increased to 100% by co-implantation with MSCs. However, the rate of liver metastasis decreased to 50% and 60%, respectively, with imatinib administration (Fig. 6*a*). The total volume of liver metastases at 4 weeks after transplantation of KM12SM cells mixed with MSCs was significantly greater than that after transplantation of KM12SM cells alone (66.7 ± 39.6 mm^3 *vs.* 345.9 ± 172 mm^3, $p < 0.05$) (Fig. 6*b*), but with imatinib administration, the total volume did not differ significantly between metastases resulting from transplantation of tumor cells alone or transplantation of mixed cells (4.7 ± 2.3 mm^3 *vs.* 28.8 ± 20.7 mm^3).

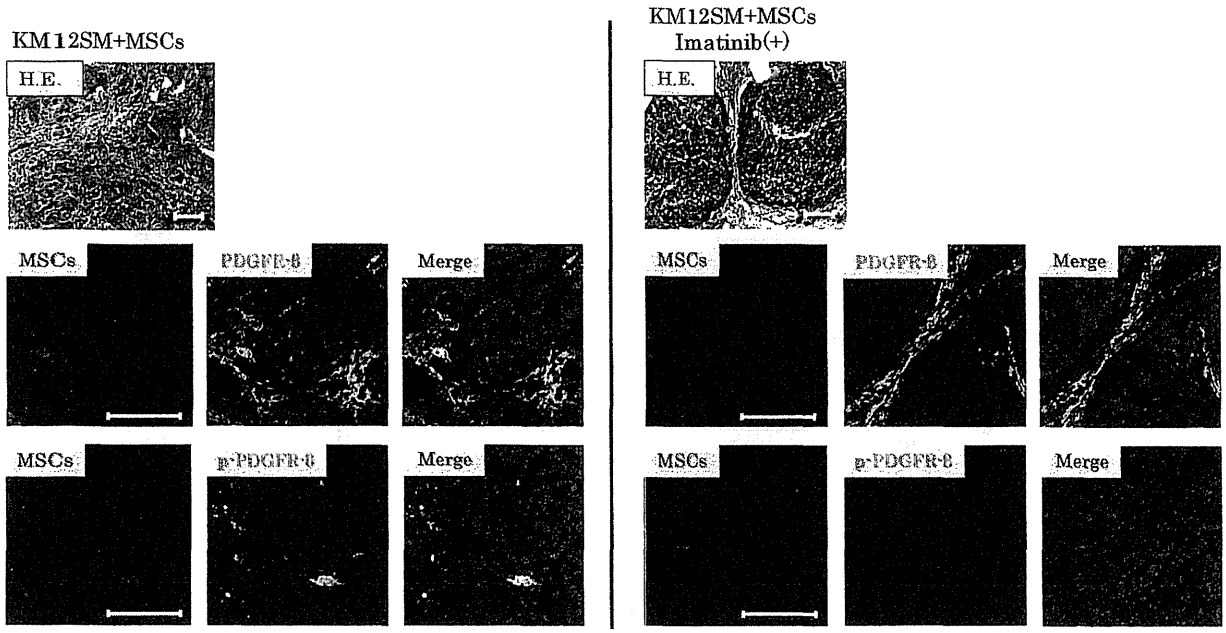

Figure 5. Phosphorylation of PDGFR-β in MSCs with or without imatinib treatment *in vivo*. PDGFR-β in MSCs was phosphorylated 3 weeks after transplantation of KM12SM cells mixed with PKH26-labeled MSCs, and it was inhibited by imatinib treatment.

Discussion

In this study, we found that tumor tropism of MSCs was inhibited by treatment with imatinib *in vivo* and *in vitro*. Oral administration of imatinib significantly inhibited the tumor growth- and metastasis-promoting effects of MSCs in our orthotopic colon cancer and liver metastasis models, and it prolonged survival of the mice. The treatment with imatinib also decreased the number of MSCs in the tumor stroma and impaired the cell proliferation- and angiogenesis-promoting effects of MSCs as well as the apoptosis-inhibiting effect of MSCs.

We previously showed in surgical specimens of human colon cancer that expression of PDGFR-β in tumor stroma is associated with vascularity and tumor stage.[5] Most cancer cells secrete PDGFs, but do not express PDGFRs, suggesting that PDGF may act as a paracrine growth factor.[41–43] In orthotopic mice models of colon and gastric cancers, PDGF-B was expressed by cancer cells, whereas PDGFR-β was expressed mainly by CAFs, and blockade of PDGFR signaling by imatinib in combination with irinotecan significantly inhibited tumor growth and metastasis.[4,8] The antitumor effects were obvious in PDGF-B high-expressing tumors in comparison with effects in PDGF-B low-expressing tumors, in which the stromal reaction is minimal. These findings indicate that PDGFR signaling in CAFs plays an important role in the growth and progression of colon carcinoma.

Paracrine activation of PDGFRs is reported to act as a potent signal for tumor stroma recruitment of fibroblasts in experimental models.[41,44] Ishii *et al.* showed that CAFs derived from human lung cancer tissue display significantly higher migratory activity in response to PDGF-B than that of fibroblasts from corresponding noncancerous tissue.[45] We recently reported functional incorporation of MSCs into the stroma of orthotopic colon tumors, where they differentiate into CAFs with high PDGFR-β expression.[34] In addition, Goldstein *et al.*[33] recently showed that endogenous MSCs can migrate from the bone to primary tumors. Molecules such as CXCL12 (SDF-1)/CXCR4,[18] CCL2 (MCP-1)/CCR2,[21] TGF-β,[33] and PDGF/PDGFR,[19] are reportedly involved in the tumor-homing ability of MSCs. The mechanisms of MSC migration seem to be complex, but among involved factors, PDGF-B is reported to be the strongest.[15,19] PDGF-B is also known to be important to the survival of MSCs transplanted *in vivo*.[36] Thus, we hypothesized that PDGFR tyrosine kinase inhibitor can impair migration of MSCs toward primary tumor as well as the tumor promoting effect of MSCs.

Although recent studies have revealed that MSCs promote tumor growth and metastasis in co-transplantation models,[22,24–31] the molecular mechanisms underlying these effects remain unclear. Our present study showed that treatment with imatinib inhibits migration and survival of MSCs in tumor stroma, suggesting the importance of the PDGF/PDGFR system in the progression of colon cancer. Treatment with imatinib impaired the tumor-promoting effect of MSCs. However, imatinib had no effect on tumor growth when cancer cells were transplanted alone, indicating that the contribution of host-derived MSCs to tumor progression was at best minimal in this model. This may be, at least in part, because these MSCs and tumor cells were derived from different species.

The PDGF/PDGFR signaling pathway is known to play an important role in increasing interstitial fluid pressure (IFP) in

a

Implanted cells	No. of mice with liver metastasis/ total no. of mice
KM12SM	7/10
KM12SM+MSCs	10/10
KM12SM Imatinib(+)	5/10
KM12SM+MSCs Imatinib(+)	6/10

N.S. N.S. N.S. N.S.

b

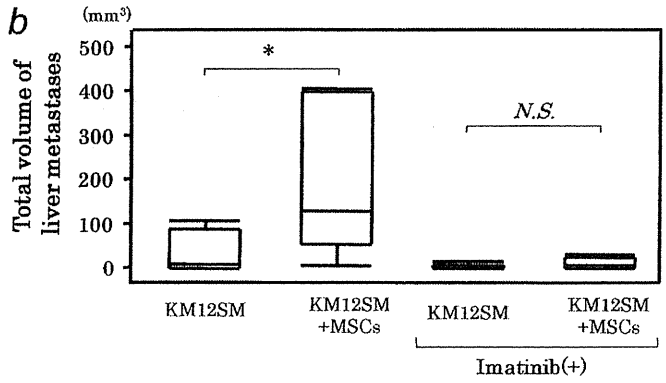

Figure 6. Formation and total volume of liver metastases in the four groups of mice. (*a*) Transplantation of KM12SM cells plus MSCs into the spleen resulted in 100% formation of liver metastases, but transplantation of KM12SM cells alone, or transplantation of KM12SM cells with or without imatinib treatment decreased the rate to 70%, 50% and 60%, respectively. (*b*) Total volume of liver metastases was significantly greater in the mixed-cell group without imatinib treatment than in other groups (each group, $n = 10$). $^*p < 0.05$, bars: SE.

tumor stroma.[40,46] Increased IFP can prevent effective distribution of antitumor drugs in the tumor microenvironment. Inhibition of the PDGF/PDGFR signaling pathway can decrease this pressure and, hence, enhance the effects of chemotherapeutic agents.[47] Our findings suggest that the tumor-inhibiting effect of imatinib may involve a reduction in CAFs derived from MSCs in the tumor microenvironment. However, imatinib is not a PDGFR-specific inhibitor; it can also inhibit the protein-tyrosine kinase activity of c-KIT, the receptor for KIT ligand, discoidin domain receptors (DDR-1 and -2), receptors for collagen, CSFR-1, the receptor for colony stimulating factors, and of ABL together with the chronic myeloid leukemia oncoprotein, BCR-ABL.[48] It has been reported that some solid tumor cell lines such as small cell lung[49] and pancreatic cancer cell lines,[50] coexpress c-Kit and Kit ligand. We recently found that cultured MSCs coexpress mRNA for c-kit and kit ligand, but there were few mononuclear cells that express c-kit and kit ligand in the xenograft resulting from transplantation of KM12SM cells mixed with MSCs (data not shown).In addition, imatinib might affect other tyrosine kinases expressed in tumor cells. Further studies are needed to clarify whether c-Kit in MSCs or other tyrosine kinases in tumor cells are involved in tumor progression *via* tumor-MSC interaction.

In addition, though we showed that MSCs promote tumor growth and metastasis in cotransplantation models, we think it would be more convincing if we could show that intravenous administration of MSCs also enhances tumor progression. In the natural setting, MSCs exist at low frequencies in human adult bone marrow, accounting for 0.00001% to 0.001% of mononuclear cells in bone marrow. However, MSCs may travel from bone marrow to tumor stroma continuously. We administered 1.0×10^6 MSCs by one-shot intravenous injection. In this model, MSCs did not promote tumor growth and metastasis (data not shown). We speculate that this is because the number of MSCs was not adequate for enhancement of tumor growth. It would be very interesting to know whether MSCs affect tumor growth if administered continuously, but if we do this in mice, they will die of pulmonary embolism. Thus, it is experimentally difficult to inject MSCs continuously as the same as a natural setting. Thus, it is experimentally difficult to mimic continuous MSC release.

Our study findings point to a possibility that migration of MSCs and the tumor-promoting effects of MSCs can be controlled by molecularly targeted antitumor drugs aimed at bone marrow-derived cells.

Acknowledgements

Cell lines were validated by STR DNA fingerprinting by means of the AmpF STR Identifier kit according to the manufacturer's instructions (Applied Biosystems catalog number 4322288). The STR profiles were compared with known ATCC fingerprints (ATCC.org) and with the Cell Line Integrated Molecular Authentication database (CLIMA) version 0.1.200808 (available at: http://bioinformatics.istge.it/clima/) (Nucleic Acids Research 37:D925-D932 PMCID: PMC2686526). The STR profiles matched known DNA fingerprints or were unique.

The authors thank Ms. Megumi Wakisaka and Mr. Shinichi Norimura for their excellent technical assistance. This work was carried out with the kind cooperation of the Analysis Center of Life Science and Institute of Laboratory Animal Science, Hiroshima University (Hiroshima, Japan).

References

1. Mantovani A, Allavena P, Sica A, et al. Cancer-related inflammation. *Nature* 2008;454:436–44.
2. Whiteside TL. The tumor microenvironment and its role in promoting tumor growth. *Oncogene* 2008;27:5904–12.
3. Kitadai Y. Cancer-stromal cell interaction and tumor angiogenesis in gastric cancer. *Cancer Microenviron* 2009.
4. Kitadai Y, Sasaki T, Kuwai T, et al. Targeting the expression of platelet-derived growth factor receptor by reactive stroma inhibits growth and metastasis of human colon carcinoma. *Am J Pathol* 2006;169:2054–65.
5. Kitadai Y, Sasaki T, Kuwai T, et al. Expression of activated platelet-derived growth factor receptor in stromal cells of human colon carcinomas is associated with metastatic potential. *Int J Cancer* 2006;119:2567–74,
6. Orimo A, Gupta PB, Sgroi DC, et al. Stromal fibroblasts present in invasive human breast carcinomas promote tumor growth and angiogenesis through elevated SDF-1/CXCL12 secretion. *Cell* 2005;121:335–48
7. De Wever O, Mareel M. Role of tissue stroma in cancer cell invasion. *J Pathol* 2003;200:429–47.
8. Sumida T, Kitadai Y, Shinagawa K, et al. Anti-stromal therapy with imatinib inhibits growth and metastasis of gastric carcinoma in an orthotopic nude mouse model. *Int J Cancer* 2010; 128:2050–62.
9. Kalluri R, Zeisberg M. Fibroblasts in cancer. *Nat Rev Cancer* 2006;6:392–401.
10. Zeisberg EM, Potenta S, Xie L, et al. Discovery of endothelial to mesenchymal transition as a source for carcinoma-associated fibroblasts. *Cancer Res* 2007;67:10123–8.
11. Direkze NC, Hodivala-Dilke K, Jeffery R, et al. Bone marrow contribution to tumor-associated myofibroblasts and fibroblasts. *Cancer Res* 2004; 64:8492–5.
12. Pittenger MF, Mackay AM, Beck SC, et al. Multilineage potential of adult human mesenchymal stem cells. *Science* 1999;284:143–7.
13. Gregory CA, Prockop DJ, Spees JL. Non-hematopoietic bone marrow stem cells: molecular control of expansion and differentiation. *Exp Cell Res* 2005;306:330–5.
14. Studeny M, Marini FC, Champlin RE, et al. Bone marrow-derived mesenchymal stem cells as vehicles for interferon-beta delivery into tumors. *Cancer Res* 2002;62:3603–8.
15. Nakamizo A, Marini F, Amano T, et al. Human bone marrow-derived mesenchymal stem cells in the treatment of gliomas. *Cancer Res* 2005;65: 3307–18.
16. Nakamura K, Ito Y, Kawano Y, et al. Antitumor effect of genetically engineered mesenchymal stem cells in a rat glioma model. *Gene Ther* 2004; 11:1155–64.
17. Hung SC, Deng WP, Yang WK, et al. Mesenchymal stem cell targeting of microscopic tumors and tumor stroma development monitored by noninvasive in vivo positron emission tomography imaging. *Clin Cancer Res* 2005;11:7749–56.
18. Menon LG, Picinich S, Koneru R, et al. Differential gene expression associated with migration of mesenchymal stem cells to conditioned medium from tumor cells or bone marrow cells. *Stem Cells* 2007;25:520–8.
19. Beckermann BM, Kallifatidis G, Groth A, et al. VEGF expression by mesenchymal stem cells contributes to angiogenesis in pancreatic carcinoma. *Br J Cancer* 2008;99:622–31.
20. Kallifatidis G, Beckermann BM, Groth A, et al. Improved lentiviral transduction of human mesenchymal stem cells for therapeutic intervention in pancreatic cancer. *Cancer Gene Ther* 2008;15:231–40.
21. Dwyer RM, Potter-Beirne SM, Harrington KA, et al. Monocyte chemotactic protein-1 secreted by primary breast tumors stimulates migration of mesenchymal stem cells. *Clin Cancer Res* 2007;13: 5020–7.
22. Karnoub AE, Dash AB, Vo AP, et al. Mesenchymal stem cells within tumour stroma promote breast cancer metastasis. *Nature* 2007; 449:557–63.
23. Klopp AH, Spaeth EL, Dembinski JL, et al. Tumor irradiation increases the recruitment of circulating mesenchymal stem cells into the tumor microenvironment. *Cancer Res* 2007;67: 11687–95.
24. Annabi B, Naud E, Lee YT, et al. Vascular progenitors derived from murine bone marrow stromal cells are regulated by fibroblast growth factor and are avidly recruited by vascularizing tumors. *J Cell Biochem* 2004;91:1146–58.
25. Djouad F, Bony C, Apparailly F, et al. Earlier onset of syngeneic tumors in the presence of mesenchymal stem cells. *Transplantation* 2006;82: 1060–6.
26. Djouad F, Plence P, Bony C, et al. Immunosuppressive effect of mesenchymal stem cells favors tumor growth in allogeneic animals. *Blood* 2003;102:3837–44.
27. Mishra PJ, Mishra PJ, Glod JW, et al. Mesenchymal stem cells: flip side of the coin. *Cancer Res* 2009;69:1255–8.
28. Mishra PJ, Mishra PJ, Humeniuk R, et al. Carcinoma-associated fibroblast-like differentiation of human mesenchymal stem cells. *Cancer Res* 2008;68:4331–9.
29. Ramasamy R, Lam EW, Soeiro I, et al. Mesenchymal stem cells inhibit proliferation and apoptosis of tumor cells: impact on in vivo tumor growth. *Leukemia* 2007;21:304–10.
30. Sun B, Zhang S, Ni C, et al. Correlation between melanoma angiogenesis and the mesenchymal stem cells and endothelial progenitor cells derived from bone marrow. *Stem Cells Dev* 2005;14: 292–8.
31. Zhu W, Xu W, Jiang R, et al. Mesenchymal stem cells derived from bone marrow favor tumor cell growth in vivo. *Exp Mol Pathol* 2006;80: 267–74.
32. Liu S, Ginestier C, Ou SJ, et al. Breast cancer stem cells are regulated by mesenchymal stem cells through cytokine networks. *Cancer Res* 2011; 71:614–24.
33. Goldstein RH, Reagan MR, Anderson K, et al. Human bone marrow-derived MSCs can home to orthotopic breast cancer tumors and promote bone metastasis. *Cancer Res* 2010;70: 10044–50.
34. Shinagawa K, Kitadai Y, Tanaka M, et al. Mesenchymal stem cells enhance growth and metastasis of colon cancer. *Int J Cancer* 2010;127: 2323–33.
35. Quante M, Tu SP, Tomita H, et al. Bone marrow-derived myofibroblasts contribute to the mesenchymal stem cell niche and promote tumor growth. *Cancer Cell* 2011;19:257–72.
36. Krausgrill B, Vantler M, Burst V, et al. Influence of cell treatment with PDGF-BB and reperfusion on cardiac persistence of mononuclear and mesenchymal bone marrow cells after transplantation into acute myocardial infarction in rats. *Cell Transplant* 2009;18:847–53.
37. Druker BJ, Lydon NB. Lessons learned from the development of an abl tyrosine kinase inhibitor for chronic myelogenous leukemia. *J Clin Invest* 2000;105:3–7.
38. Ishii M, Koike C, Igarashi A, et al. Molecular markers distinguish bone marrow mesenchymal stem cells from fibroblasts. *Biochem Biophys Res Commun* 2005;332:297–303.
39. Morikawa K, Walker SM, Nakajima M, et al. Influence of organ environment on the growth, selection, and metastasis of human colon carcinoma cells in nude mice. *Cancer Res* 1988; 48:6863–71.
40. Hwang RF, Yokoi K, Bucana CD, et al. Inhibition of platelet-derived growth factor receptor phosphorylation by STI571 (Gleevec) reduces growth and metastasis of human pancreatic carcinoma in an orthotopic nude mouse model. *Clin Cancer Res* 2003;9:6534–44.
41. Forsberg K, Valyi-Nagy I, Heldin CH, et al. Platelet-derived growth factor (PDGF) in oncogenesis: development of a vascular connective tissue stroma in xenotransplanted human melanoma producing PDGF-BB. *Proc Natl Acad Sci USA* 1993;90:393–7.
42. Micke P, Ostman A. Tumour-stroma interaction: cancer-associated fibroblasts as novel targets in anti-cancer therapy? *Lung Cancer* 2004;45(Suppl 2):S163–75.
43. Paulsson J, Sjoblom T, Micke P, et al. Prognostic significance of stromal platelet-derived growth factor beta-receptor expression in human breast cancer. *Am J Pathol* 2009;175:334–41.

44. Skobe M, Fusenig NE. Tumorigenic conversion of immortal human keratinocytes through stromal cell activation. *Proc Natl Acad Sci USA* 1998;95: 1050–5.
45. Ishii G, Hashimoto H, Asada K, et al. Fibroblasts associated with cancer cells keep enhanced migration activity after separation from cancer cells: a novel character of tumor educated fibroblasts. *Int J Oncol* 2010; 37:317–25.
46. Pietras K, Ostman A, Sjoquist M, et al. Inhibition of platelet-derived growth factor receptors reduces interstitial hypertension and increases transcapillary transport in tumors. *Cancer Res* 2001;61:2929–34.
47. Pietras K. Increasing tumor uptake of anticancer drugs with imatinib. *Semin Oncol* 2004;31:18–23.
48. Manley PW, Stiefl N, Cowan-Jacob SW, et al. Structural resemblances and comparisons of the relative pharmacological properties of imatinib and nilotinib. *Bioorg Med Chem* 2010;18:6977–86.
49. Hibi K, Takahashi T, Sekido Y, et al. Coexpression of the stem cell factor and the c-kit genes in small-cell lung cancer. *Oncogene* 1991;6: 2291–6.
50. Yasuda A, Sawai H, Takahashi H, et al. The stem cell factor/c-kit receptor pathway enhances proliferation and invasion of pancreatic cancer cells. *Mol Cancer* 2006;5:46.

Expression of *miR-486* is a potential prognostic factor after nephrectomy in advanced renal cell carcinoma

KEISUKE GOTO[1,2], NAOHIDE OUE[1], SHUNSUKE SHINMEI[1,2], KAZUHIRO SENTANI[1], NAOYA SAKAMOTO[1], YUTAKA NAITO[1], TETSUTARO HAYASHI[2], JUN TEISHIMA[2], AKIO MATSUBARA[2] and WATARU YASUI[1]

Departments of [1]Molecular Pathology and [2]Urology, Hiroshima University Institute of Biomedical and Health Sciences, Hiroshima 734-8551, Japan

Received October 3, 2012; Accepted November 6, 2012

DOI: 10.3892/mco.2012.46

Abstract. Renal cell carcinoma is the most frequently occurring neoplasm in the adult kidney, leading to poor prognosis. Therefore novel biomarkers are required for the prediction of early metastasis following nephrectomy. The aim of the present study was to investigate whether or not expression levels of *miR-486*, detected in RNA isolated from formalin-fixed paraffin-embedded tissue sections, can predict prognosis for patients with renal cell carcinoma (RCC). Expression levels of *miR-486* were measured by quantitative reverse transcriptase-polymerase chain reaction in 150 RCC cases. Expression of *miR-486* in RCC samples was ~2.7-fold higher than in corresponding non-neoplastic kidney samples (P<0.0001). In stage III and IV RCC cases (n=46), a high *miR-486* expression in tumors was associated with worse cancer-specific mortality, independent of clinical covariates, including TNM staging (P=0.0064). In addition, *miR-486* expression tended to be associated with cancer-specific mortality in stage III and IV RCC patients who were not treated with interferon-α (Kaplan-Meier analysis, n=14, P=0.0574). These results suggest that *miR-486* is a promising biomarker to identify poor prognosis in RCC patients. As expression of *miR-486* was measured from formalin-fixed paraffin-embedded (FFPE) samples, this study demonstrated that measurement of *miR-486* may be readily translated into clinical applications.

Introduction

Renal cell carcinoma (RCC) is the most common neoplasm in the adult kidney and accounts for 2-3% of malignant diseases in adults. Locally extensive or metastatic RCC, even following complete resection, have worse prognoses compared to organ-confined diseases. Therefore, there is a need to identify novel biomarkers that enable prediction of early metastasis after nephrectomy, and to develop novel targeted therapies.

Cancer develops as a result of multiple genetic and epigenetic alterations. Better knowledge of changes in gene expression that occur during carcinogenesis may lead to improvements in diagnosis, treatment and prevention. Potential biomarkers identifying high-risk patients have been reported, however, assessment methods for these biomarkers often involve RNA-based techniques and require fresh frozen tissues. By contrast, formalin-fixed paraffin-embedded (FFPE) tissue samples have been collected during decades of routine histopathological examination and those are the most widely available materials in clinical use. However, formaldehyde-containing fixatives cause cross-linkage between nucleic acids and proteins, rendering subsequent extraction and quantification of RNA challenging (1). A major obstacle to RNA expression analysis of FFPE tissues has been the uncertainty as to whether or not gene expression analyses from routinely archived tissues accurately reflect the expression levels prior to fixation, since the fixation process is likely to cause a high degree of RNA fragmentation (2). Given that naturally occurring small RNAs are not affected by fragmentation and therefore do not experience loss of quality, targeting miRNAs is more suitable for analysis of RNA extracted from FFPE samples.

miRNAs are 18- to 25-nucleotide, non-coding RNA molecules that regulate the translation of several genes (3). miRNA expression levels are altered in most types of human cancers (4-6). Several RCC studies have examined miRNAs by microarray analysis using a relatively small amount of frozen tissue samples. Various miRNAs that are dysregulated in RCC have been identified (7,8). Several lines of evidence indicate that *miR-486* has oncogenic properties. Overexpression of *miR-486* has been reported in cutaneous T-cell lymphoma (9). High serum or plasma expression levels of *miR-486* have been reported in non-small cell lung (10) and gastric cancers (11). *miR-486* has also been reported to target *PTEN* and *FOXO1*, which negatively affect PI3K/Akt signaling (12). The Akt-signaling pathway functions as a potent activator of growth and survival signaling (13). However, expression of *miR-486* has not been investigated in RCC.

In the present study, we investigated the association of *miR-486* expression with RCC patient prognosis (n=150) using

Correspondence to: Professor Wataru Yasui, Department of Molecular Pathology, Hiroshima University Institute of Biomedical and Health Sciences, 1-2-3 Kasumi, Minami-ku, Hiroshima 734-8551, Japan
E-mail: wyasui@hiroshima-u.ac.jp

Key words: miRNA, *miR-486*, renal cell carcinoma, prognosis

quantitative reverse transcription polymerase chain reaction (qRT-PCR) of FFPE samples. In addition, since it has been reported that *olfactomedin 4 (OLFM4)*, which encodes the olfactomedin 4 protein, is one of the direct targets of *miR-486* (14), immunohistochemical analysis of olfactomedin 4 was carried out in RCC tissues.

Materials and methods

Tissue samples. In a retrospective study design, 150 primary tumors were collected consecutively from patients diagnosed with RCC who underwent surgery between 2001 and 2008 at the Hiroshima University Hospital (Hiroshima, Japan). Only patients without preoperative radiotherapy or chemotherapy were enrolled in the study. Of 150 patients, 129 were at stages I, II and III, while 21 were at stage IV. The 129 patients with stage I, II and III RCC underwent curative resection. Of the 129 patients with stage I, II and III RCC, 20 received adjuvant therapy (interferon-α) (15). Of the 21 patients with stage IV RCC, 17 received postoperative therapy using interferon-α (15). Postoperative follow-up was scheduled every 1, 2 or 3 months during the first 2 years after surgery, and every 6 months thereafter unless more frequent follow-up was deemed necessary. Chest-abdominal computed tomography scan and serum chemistries were performed during each 6 month visit at least. Patients were monitored by their physician until they succumbed to the disease or the date of the last documented contact. The median follow-up period was 64 months (range, 2-120). Operative mortality was defined as death within 30 days of the patient leaving the hospital, and these patients were omitted from the analysis.

For qRT-PCR analysis, archival FFPE tissues were used. Histological classification was based on the World Health Organization system. RCC cases were classified into clear cell RCC (ccRCC) and non-ccRCC. Tumor staging was performed according to the TNM grouping system. Since written informed consent was not obtained, for reasons of strict privacy protection, identifying information for the samples was removed prior to analysis. This procedure was in accordance with the Ethical Guidelines for Human Genome/Gene Research of the Japanese Government.

RNA extraction and qRT-PCR. FFPE samples were sectioned (10 μm), deparaffinized and stained with hematoxylin and eosin (H&E) to ensure that the sectioned block contained tumor cells. The tumor areas in the adjacent sections were marked under a light microscope without hematoxylin staining. Tumor areas were macrodissected with sterile disposable scalpels and subjected to RNA isolation using the Recover All™ Total Nucleic Acid Isolation kit (Ambion, Austin, TX, USA), according to the manufacturer's instructions. Expression levels of *miR-486* and *RNU6B* were measured using TaqMan® assays for miRNA (Applied Biosystems, Austin, TX, USA) in such a manner that the identity and clinical outcomes of samples were blinded. Complementary DNA (cDNA) was synthesized using miRNA-specific primers and the TaqMan® MicroRNA Reverse Transcription kit (Applied Biosystems) according to the manufacturer's instructions. Briefly, 40 ng of RNA was reverse transcribed in a 20 μl reaction with gene-specific RT probes. qRT-PCR was performed using the ABI 7900 Version 2.3 Sequence Detection System (Applied Biosystems). *RNU6B* was used as an endogenous normalization control for *miR-486*. The assays were performed in triplicate. Quantification of *miR-486* relative expression was calculated using the RQ manager 1.2 (Applied Biosystems).

Table I. Association between *miR-486* expression and clinicopathological characteristics.

	miR-486 expression		
Characteristics	High (%)	Low	P-value
Age (years)			
<66	48 (69)	22	0.1084
≥66	64 (80)	16	
Gender			
Male	80 (73)	29	0.5552
Female	32 (78)	9	
T classification			
1	71 (77)	21	0.5009
2	12 (71)	5	
3	27 (69)	12	
4	2 (100)	0	
N classification			
0	107 (76)	34	0.4049
1	2 (50)	2	
2	3 (60)	2	
M classification			
0	98 (75)	32	0.6119
1	14 (70)	6	
Tumor stage			
I	71 (79)	19	0.1792
II	10 (71)	4	
III	16 (67)	8	
IV	15 (68)	7	
Histological classification			
ccRCC	101 (74)	36	0.3649
Non-ccRCC	11 (85)	2	
Venous invasion			
Positive	35 (74)	12	0.9699
Negative	77 (75)	26	
Interferon-α treatment			
Received	23 (62)	14	0.0519
Not received	89 (79)	24	

ccRCC, clear cell renal cell carcinoma.

Immunohistochemistry. FFPE samples were sectioned, deparaffinized and stained with H&E to ensure that the sectioned block contained tumor cells. Adjacent sections were then stained immunohistochemically with the Dako EnVision+ Mouse Peroxidase Detection System (DakoCytomation, Carpinteria, CA, USA). Antigen retrieval

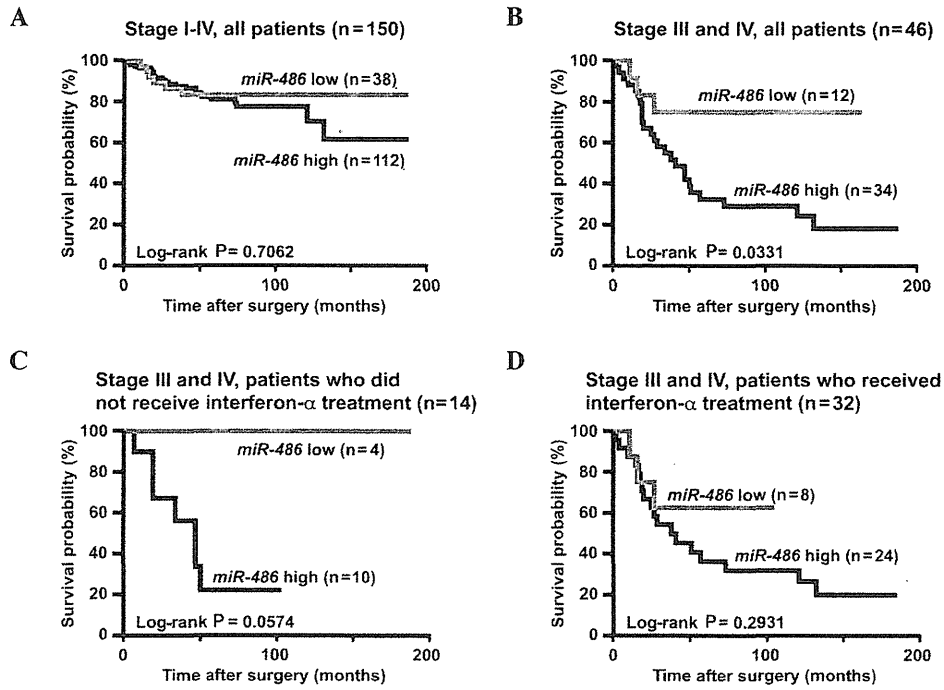

Figure 1. (A) Kaplan-Meier curves of *miR-486*-high or -low renal cell carcinoma (RCC) in stage I-IV patients. Cancer-specific mortality did not statistically vary in high- and low-miR-486 cases. (B) Kaplan-Meier curves of *miR-486*-high or -low RCC in stage III and IV patients. High-miR-486 expression had significantly worse cancer-specific mortality compared to those with low-miR-486 expression. (C) Kaplan-Meier curves of *miR-486*-high or -low RCC in stage III and IV patients who did not receive interferon-α treatment. Cancer-specific mortality of patients with high-miR-486 expression tended to be worse compared to that of patients with low-miR-486 expression. (D) Kaplan-Meier curves of *miR-486*-high or -low RCC in stage III and IV patients who received interferon-α treatment. Expression of miR-486 was not significantly associated with therapeutic outcome.

was performed by microwave heating in citrate buffer (pH 6.0) for 30 min. After peroxidase activity was blocked with 3% H_2O_2 methanol for 10 min, sections were incubated with normal goat serum (DakoCytomation) for 20 min to block non-specific antibody binding sites. Sections were incubated with primary antibodies against olfactomedin 4 (1:50 dilution, using an anti-olfactomedin 4 antibody raised in our laboratory) (16) for 1 h at room temperature, followed by incubations with EnVision+ anti-mouse peroxidase for 1 h. Staining was completed with 10-min incubation with the substrate-chromogen solution. Sections were counterstained using 0.1% hematoxylin.

Statistical analysis. Associations between clinicopathological characteristics and *miR-486* expression were analyzed using the Fisher's exact test. To evaluate the associations between clinical covariates and cancer-specific mortality univariate and multivariate Cox regression analysis was used and conducted using SPSS software (SPSS Inc., Chicago, IL, USA). Hazard ratio (HR) and 95% confidence interval (CI) were estimated from the Cox proportional hazard models. For the analyses, age was treated as a categorical variable (65 plus >65 vs. <65 years old). For the final multivariate Cox regression models, the variables that were moderately associated (P<0.10) with cancer-specific mortality were included. Differences in *miR-486* expression levels between the two groups were determined by the Mann-Whitney U test using Graphpad Prism 5.0 (Graphpad Software, Inc., San Diego, CA, USA). Kaplan-Meier survival curves were constructed for high- and low-*miR-486* patients using the Graphpad Prism 5.0 software. Differences between survival curves were tested for statistical significance using the log-rank test. P<0.05 was considered to indicate a statistically significant difference.

Results

Expression of miR-486 in RCC and non-neoplastic kidney tissue. The expression of *miR-486* and the corresponding non-neoplastic kidney tissue samples were assessed in 86 RCC cases using qRT-PCR. The expression of *miR-486* in RCC samples was ~2.7-fold higher compared to that in corresponding non-neoplastic kidney samples (P<0.0001, Mann-Whitney U-test).

Association between miR-486 expression levels and clinicopathological characteristics. Expression of *miR-486* was examined in 64 additional RCC tissue samples using qRT-PCR. We investigated the association between the clinicopathological characteristics and *miR-486* expression levels in 150 RCC cases (Table I). These 150 RCC cases were divided into high- and low-*miR-486* cases. When low-*miR-486* expression was classified according to the lowest quartile, the number of high- and low-*miR-486* cases was 112 and 38, respectively. Expression of *miR-486* was not associated with clinicopathological characteristics such as gender, T, N and M classifications, tumor stage or venous invasion.

Association between miR-486 expression and survival. The association between *miR-486* expression levels and cancer-specific mortality was evaluated. The Kaplan-Meier analysis for the 150 RCC cases (stages I-IV) was performed.

Table II. Univariate and multivariate Cox regression analysis of *miR-486* expression and cancer-specific mortality in stage III and IV RCC.

	Univariate analysis		Multivariate analysis	
Characteristics	HR (95% CI)	P-value	HR (95% CI)	P-value
Age (years)				
<66	1 (Ref.)	0.5719		
≥66	1.24 (0.58-2.66)			
Gender				
Male	1 (Ref.)	0.5919		
Female	0.73 (0.17-2.08)			
Histological classification				
Non-ccRCC	1 (Ref.)	0.5714		
ccRCC	0.64 (0.18-4.00)			
Venous invasion				
Negative	1 (Ref.)	0.9318		
Positive	1.04 (0.42-3.10)			
T classification				
1/2	1 (Ref.)	0.8861		
3/4	1.09 (0.37-4.60)			
N classification				
0	1 (Ref.)	0.0315	1 (Ref.)	0.9832
1/2	2.73 (1.10- 6.24)		1.01 (0.32-2.89)	
M classification				
0	1 (Ref.)	0.0035	1 (Ref.)	0.2398
1	3.16 (1.46-7.08)		0.31 (0.05-2.47)	
Tumor stage				
III	1 (Ref.)	0.0005	1 (Ref.)	0.0386
IV	4.03 (1.82-9.54)		9.72 (1.14-59.82)	
Interferon-α treatment				
Not received	1 (Ref.)	0.5558		
Received	1.28 (0.57-3.28)			
miR-486 expression				
Low	1 (Ref.)	0.0202	1 (Ref.)	0.0064
High	3.38 (1.18-14.26)		4.33 (1.45-18.71)	

RCC, renal cell carcinoma; ccRCC, clear cell RCC; HR, hazard ratio; CI, confidence interval.

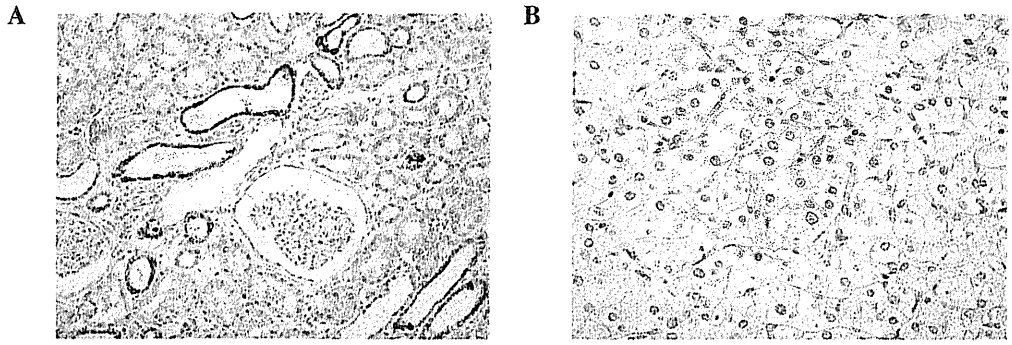

Figure 2. Immunohistochemical analysis of olfactomedin 4. (A) In non-neoplastic kidney, olfactomedin 4 staining was observed in uriniferous tubule but not glomerulus (original magnification, x200). (B) In renal cell carcinoma, olfactomedin 4 staining was not present (original magnification, x400).

As shown in Fig. 1A, cancer-specific mortality did not statistically vary in high- and low-*miR-486* cases.

Patients with RCC at stage I and II have a good rate of survival, whereas it is difficult to predict patient survival with stage III and IV RCC. These patients would benefit greatly from prognostic biomarkers. Therefore, we analyzed the prognostic value of *miR-486* expression in patients with stage III and IV RCC (n=46). Using the Kaplan-Meier analysis, we found that RCC cases with high-*miR-486* expression had significantly worse cancer-specific mortality compared to those with low-*miR-486* expression (P=0.0331, log-rank test, Fig. 1B). Since treatment with interferon-α for patients with stage III and IV RCC may affect patient survival, individuals who did not receive interferon-α treatment (n=14) were assessed. Although cancer-specific mortality among patients with high- and low-*miR-486* expression exhibited no statistically significant difference (P=0.0574, log-Rank test, Fig. 1C), cancer-specific mortality of patients with high-*miR-486* expression tended to be worse compared to that of patients with low-*miR-486* expression.

To evaluate the potential for *miR-486* expression as a prognostic predictor in patients with stage III and IV RCC, univariate and multivariate Cox proportional hazards analyses were used to evaluate the association of *miR-486* expression with cancer-specific mortality (Table II). Findings of the univariate analysis showed that N (HR, 2.73; 95% CI, 1.10-6.24; P=0.0315) and M classifications (HR, 3.16; 95% CI, 1.46-7.08; P=0.0035), tumor stage (HR, 4.03; 95% CI, 1.82-9.54; P=0.0005) and *miR-486* expression (HR, 3.38; 95% CI, 1.18-14.26; P=0.0202) were significantly associated with cancer-specific mortality. According to the multivariate model, which included N and M classifications, tumor stage and *miR-486* expression, expression of *miR-486* was an independent prognostic classifier of cancer-specific mortality (HR, 4.33; 95% CI, 1.45-18.71; P=0.0064).

Survival analysis was performed using an alternatively defined cut-off point. When low-*miR-486* expression was defined on the basis of lower than median levels of expression of *miR-486*, the number of high- as well as low-*miR-486* *miR-486* cases was 75. Kaplan-Meier analysis revealed that cancer-specific mortality did not exhibit statistically significant differences in high- and low-*miR-486* cases (data not shown). When low-*miR-486* expression was classified according to the lowest tertile, the number of high- and low-*miR-486* cases was 100 and 50, respectively. Kaplan-Meier analysis revealed that cancer-specific mortality did not exhibit statistically significant differences in high- and low-*miR-486* cases (data not shown).

Expression of miR-486 and therapeutic outcomes. Biomarkers that predict therapeutic outcomes may provide tools to allow physicians to better stratify patients to more effective treatments. Therefore, we analyzed the association between *miR-486* expression and therapeutic outcomes in stage III and IV RCC patients treated with interferon-α (n=32). However, expression of *miR-486* was not significantly associated with therapeutic outcome (P=0.2931, log-rank test, Fig. 1D).

Expression of OLFM4 in RCC. OLFM4, which encodes the OLFM4 protein, has been reported as one of the direct targets of *miR-486* (14). Although alteration of OLFM4 expression has been reported in several types of human cancer (16-18), expression of OLFM4 in RCC has not been investigated. Therefore, the expression of OLFM4 was analyzed using immunohistochemistry in 86 RCC cases. In non-neoplastic kidney, OLFM4 staining was observed in uriniferous tubules but not in glomeruli (Fig. 2A). By contrast, OLFM4 staining was not expressed in RCC cells (Fig. 2B). No OLFM4 staining was detectable in the 86 RCC cases.

Discussion

Several lines of evidence have suggested that miRNAs are useful as biomarkers as well as therapeutic targets for cancer. Prediction of the survival of patients with stage III and IV RCC remains difficult, and these groups would benefit from the detection of prognostic markers that identify individuals for whom adjuvant or post-operative treatment would be advantageous. In the present study, RNA from 150 FFPE RCC tissues was prepared, since biomarkers developed from FFPE samples may be more readily translated into clinical application. Expression of *miR-486* in patients with stage III and IV RCC was significantly associated with cancer-specific mortality according to a Kaplan-Meier analysis. The univariate and multivariate Cox proportional hazards analyses demonstrated that expression of *miR-486* was an independent prognostic classifier. Furthermore, since treatment with interferon-α for patients with stage III and IV RCC affects patient survival, individuals who did not receive interferon-α treatment were assessed. Although cancer-specific mortality among patients with high- and low-*miR-486* expression showed no statistically significant difference, cancer-specific mortality of patients with high-*miR-486* expression tended to be worse compared to that of patients with low-*miR-486* expression. This finding suggests that *miR-486* expression is associated with a more aggressive RCC histology. Taken together, these results indicate that *miR-486* is a promising biomarker to identify patients with poor prognosis in stage III and IV RCC.

In the present study, we demonstrated that *miR-486* expression was associated with cancer-specific mortality in patients with stage III and stage IV RCC. In addition, *miR-486* expression was associated with cancer-specific mortality in stage III and IV RCC patients who were not treated with interferon-α. Therefore, measurement of *miR-486* expression may help identify patients with a high risk of disease recurrence, while treatment with interferon-α may be indicative for patients with *miR-486*-positive RCC. However, it is unclear whether such patients may benefit from interferon-α treatment. To address this issue, we examined whether or not *miR-486* expression was able to identify patients for whom interferon-α treatment is beneficial in stage III and IV RCC. However, expression of *miR-486* was not significantly associated with therapeutic outcome. These results suggest that even when patients with a high risk of disease recurrence are identified by *miR-486* measurement, those patients may not benefit from interferon-α treatment. Novel therapeutic methods may be more effective for these patients.

miR-486 has been reported to have oncogenic properties. Overexpression of *miR-486* has been reported in several human malignancies. In the present study, although expression of *miR-486* in RCC samples was significantly higher compared

to that in corresponding non-neoplastic kidney samples, expression of *miR-486* was not associated with tumor stage. Therefore, high-*miR-486* expression is likely to be involved in carcinogenesis, but not in tumor progression. Since targets of *miR-486* are *PTEN* and *FOXO1* (12), expression of *PTEN* and *FOXO1* may be low in high-*miR-486* RCC cases. In addition to *PTEN* and *FOXO1*, one of the targets of *miR-486* is *OLFM4* (14). In the present study, although OLFM4 staining was observed in uriniferous tubules, staining of OLFM4 was not detected in the 86 RCC cases. Previously, we showed that patients with OLFM4-positive gastric cancer had a better survival rate compared to patients with OLFM4-negative gastric cancer (16). Forced expression of OLFM4 has also been reported to decrease cell adhesion and migration (17,18). Taken together, OLFM4 is likely to have tumor suppressive properties in RCC. Given that staining of OLFM4 was not detected in the 86 RCC cases, overexpression of *miR-486* is unlikely to have a major role in the loss of OLFM4.

In summary, we showed that a high-*miR-486* expression is an independent prognostic classifier in stage III and IV RCC. Therefore, measurement of *miR-486* helps identify high-risk patients. In this study, expression of *miR-486* from FFPE samples was assessed. Therefore, measurement of *miR-486* can be readily translated into clinical applications.

Acknowledgements

This study was supported in part by grants-in-aid for Cancer Research from the Ministry of Education, Culture, Science, Sports and Technology of Japan and in part by a grant-in-aid for the Third Comprehensive 10-Year Strategy for Cancer Control from the Ministry of Health, Labor and Welfare of Japan. The authors would like to thank Mr. Shinichi Norimura for his excellent technical assistance and advice. This study was conducted in collaboration with the Research Center for Molecular Medicine of the Faculty of Medicine of Hiroshima University. We also thank the Analysis Center of Life Science of Hiroshima University for the use of their facilities.

References

1. Srinivasan M, Sedmak D and Jewell S: Effect of fixatives and tissue processing on the content and integrity of nucleic acids. Am J Pathol 161: 1961-1971, 2002.
2. Specht K, Richter T, Muller U, Walch A, Werner M and Hofler H: Quantitative gene expression analysis in microdissected archival formalin-fixed and paraffin-embedded tumor tissue. Am J Pathol 158: 419-429, 2001.
3. Huntzinger E and Izaurralde E: Gene silencing by microRNAs: contributions of translational repression and mRNA decay. Nat Rev Genet 12: 99-110, 2011.
4. Lu J, Getz G, Miska EA, *et al*: MicroRNA expression profiles classify human cancers. Nature 435: 834-838, 2005.
5. Schetter AJ, Heegaard NH and Harris CC: Inflammation and cancer: interweaving microRNA, free radical, cytokine and p53 pathways. Carcinogenesis 31: 37-49, 2010.
6. Ueda T, Volinia S, Okumura H, *et al*: Relation between microRNA expression and progression and prognosis of gastric cancer: a microRNA expression analysis. Lancet Oncol 11: 136-146, 2010.
7. Gottardo F, Liu CG, Ferracin M, *et al*: Micro-RNA profiling in kidney and bladder cancers. Urol Oncol 25: 387-392, 2007.
8. White NM, Bao TT, Grigull J, *et al*: miRNA profiling for clear cell renal cell carcinoma: biomarker discovery and identification of potential controls and consequences of miRNA dysregulation. J Urol 186: 1077-1083, 2011.
9. Narducci MG, Arcelli D, Picchio MC, *et al*: MicroRNA profiling reveals that miR-21, miR486 and miR-214 are upregulated and involved in cell survival in Sézary syndrome. Cell Death Dis 2: e151, 2011.
10. Hu Z, Chen X, Zhao Y, *et al*: Serum microRNA signatures identified in a genome-wide serum microRNA expression profiling predict survival of non-small-cell lung cancer. J Clin Oncol 28: 1721-1726, 2010.
11. Konishi H, Ichikawa D, Komatsu S, *et al*: Detection of gastric cancer-associated microRNAs on microRNA microarray comparing pre- and post-operative plasma. Br J Cancer 106: 740-747, 2012.
12. Small EM, O'Rourke JR, Moresi V, *et al*: Regulation of PI3-kinase/Akt signaling by muscle-enriched microRNA-486. Proc Natl Acad Sci USA 107: 4218-4223, 2010.
13. Crackower MA, Oudit GY, Kozieradzki I, *et al*: Regulation of myocardial contractility and cell size by distinct PI3K-PTEN signaling pathways. Cell 110: 737-749, 2002.
14. Oh HK, Tan AL, Das K, *et al*: Genomic loss of miR-486 regulates tumor progression and the OLFM4 antiapoptotic factor in gastric cancer. Clin Cancer Res 17: 2657-2667, 2011.
15. Medical Research Council Renal Cancer Collaborators: Interferon-alpha and survival in metastatic renal carcinoma: early results of a randomised controlled trial. Medical Research Council Renal Cancer Collaborators. Lancet 353: 14-17, 1999.
16. Oue N, Sentani K, Noguchi T, *et al*: Serum olfactomedin 4 (GW112, hGC-1) in combination with Reg IV is a highly sensitive biomarker for gastric cancer patients. Int J Cancer 125: 2383-2392, 2009.
17. Koshida S, Kobayashi D, Moriai R, Tsuji N and Watanabe N: Specific overexpression of OLFM4(GW112/HGC-1) mRNA in colon, breast and lung cancer tissues detected using quantitative analysis. Cancer Sci 98: 315-320, 2007.
18. Liu W, Liu Y, Zhu J, Wright E, Ding I and Rodgers GP: Reduced hGC-1 protein expression is associated with malignant progression of colon carcinoma. Clin Cancer Res 14: 1041-1049, 2008.

INTERNATIONAL JOURNAL OF UROLOGY

International Journal of Urology (2013) 20, 468–477 doi: 10.1111/j.1442-2042.2012.03182.x

Original Article: Clinical Investigation

MicroRNA-155 is a predictive marker for survival in patients with clear cell renal cell carcinoma

Shunsuke Shinmei,[1,2] Naoya Sakamoto,[1] Keisuke Goto,[1,2] Kazuhiro Sentani,[1] Katsuhiro Anami,[1] Tetsutaro Hayashi,[2] Jun Teishima,[2] Akio Matsubara,[2] Naohide Oue,[1] Yasuhiko Kitadai[3] and Wataru Yasui[1]

Departments of [1]Molecular Pathology, [2]Urology and [3]Medicine and Molecular Science, Hiroshima University Graduate School of Biomedical Sciences, Hiroshima, Japan

Abbreviations & Acronyms
AJCC = American Joint Committee on Cancer
ccRCC = clear cell renal cell carcinoma
cDNA = complementary deoxyribonucleic acid
CFS = cancer-free survival
CI = confidence intervals
CSS = cancer-specific survival
FFPE = formalin fixed paraffin embedded
HIF-1α = hypoxia-inducible factor-1α
HR = hazard ratio
IFN-α = interferon-α
IHC = immunohistochemistry
miRNA = micro-ribonucleic acid
NS = not significant
PI3K = phosphoinositide 3-kinase
qRT–PCR = quantitative reverse transcription polymerase chain reaction
RCC = renal cell carcinoma
RNA = ribonucleic acid
SE = standard error

Correspondence: Wataru Yasui M.D., Ph.D., Department of Molecular Pathology, Hiroshima University Graduate School of Biomedical Sciences, 1-2-3 Kasumi, Minami-ku, Hiroshima 734-8551, Japan. Email: wyasui@hiroshima-u.ac.jp

Received 9 March 2012; accepted 5 September 2012. Online publication 10 October 2012

Objectives: To investigate the clinical significance of micro-ribonucleic acid-155 in clear cell renal cell carcinoma, in particular focusing on the association of expression levels of micro-ribonucleic acid-155 with clinicopathological factors, cancer-specific survival and therapeutic outcomes in clear cell renal cell carcinoma patients.

Methods: Quantitative reverse transcription polymerase chain reaction of micro-ribonucleic acid-155 was carried out on 137 clear cell renal cell carcinoma cases, containing 77 matched pairs of clear cell renal cell carcinoma and normal adjacent kidney tissues from the same patients.

Results: Significant overexpression of micro-ribonucleic acid-155 was found in clear cell renal cell carcinoma compared with normal kidney tissue. Expression of micro-ribonucleic acid-155 was not associated with prognosis in all stage groups. However, in 43 patients with stage III and IV clear cell renal cell carcinoma, low expression levels of micro-ribonucleic acid-155 correlated with a poor prognosis. Regarding cancer-free survival of 26 patients with stage III and IV clear cell renal cell carcinoma who received curative resection and cancer-specific survival of 31 patients who received postoperative therapy with interferon-α after radical nephrectomy, low expression levels of micro-ribonucleic acid-155 correlated with poor clinical outcomes in these two groups.

Conclusions: Low expression of micro-ribonucleic acid-155 represents a valuable marker of poor clinical outcomes in patients with stage III and IV clear cell renal cell carcinoma.

Key words: hypoxia-inducible factor-1α, micro-ribonucleic acid, micro-ribonucleic acid-155, quantitative reverse transcript polymerase chain reaction, renal cell carcinoma.

Introduction

RCC is the most common neoplasm of the adult kidney and the incidence is increasing worldwide, and the most common subtype is ccRCC.[1] If detected early, ccRCC can be treated surgically, and 5-year survival rates approaching 85% can be achieved for patients with organ-confined disease.[2] In reality, 40–50% of patients develop metastatic disease; 20–30% present with metastases, and 20–30% relapse distantly after curative nephrectomy. Treatment options for these patients are limited, and expected 5-year survival is approximately 10%.[2] Therefore, it is necessary to identify new biomarkers enabling prediction of early metastasis after nephrectomy and to develop new targeted therapies.

MiRNA are short non-coding RNA of 18–25 nucleotides in length that regulate gene expression post-transcriptionally. Aberrant miRNA expression is reported in many cancers, suggesting that they have a novel role as oncogenes or tumor suppressors.[3–5] Recent evidence showed the diverse clinical uses of miRNA for cancer as diagnostic, prognostic and predictive markers.[6] Differential expression of miRNA has been investigated in RCC. MiR-122, miR-155, miR-21, miR-106a, miR-182, miR-106b and miR-210 have been

reported to be overexpressed in RCC, whereas miR-141, miR-200c, miR-335 and miR-218 are downregulated.[7–15] MiR-155 has repeatedly been identified through miRNA microarray profiling as upregulated in RCC tissue and its biological role has been studied.[11,12] A significant correlation was found between miR-155 expression and tumor size.[7,8,16] Although miR-155 correlates with prognosis in breast cancer, lung cancer, hepatocellular carcinoma, colorectal cancer and pancreatic tumors,[17–21] there is only one report examining the correlation between miR-155 and prognosis in ccRCC, which was analyzed in just 31 cases and showed no prognostic impact of miR-155.[8] To confirm the correlation between miR-155 and prognosis of ccRCC patients, more validation studies in large sample sets should be carried out.

In the present study, we analyzed expression levels of miR-155 in 137 ccRCC cases by qRT–PCR, and compared these to the expression levels from 77 corresponding normal kidney tissue samples. Furthermore, the associations between expression levels of miR-155 and clinicopathological factors including prognosis were also investigated.

Methods

Tissue samples

In total, 137 primary tumor samples and 77 normal adjacent samples were collected from patients diagnosed with ccRCC. Patients were treated at the Hiroshima University Hospital from 1993 to 2010. Some cases, from a single institution, that did not have available tissue and clinical information about postoperative follow up were excluded.

Clinical stage was determined according to the AJCC Cancer Staging Manual, 7th edition. Patient's ages ranged between 34 and 89 years, with a median of 66 years. Histological diagnosis was established according to the guidelines of the World Health Organization. Cases were selected according to tissue availability and were not stratified for any known preoperative or pathological prognostic factor. The median follow-up time for all cases was 65 months and ranged from 2 to 188 months. We measured tumor sizes in 123 ccRCC tissue samples that could be confirmed macroscopically in pathological samples.

Because written informed consent was not obtained, for strict privacy protection the identifying information for all samples was removed before analysis. This procedure was in accordance with the Ethical Committee for Human Genome Research of Hiroshima University (Hiroshima, Japan). Clinical details of the patients are summarized in Table 1. We analyzed 43 samples to confirm stage III and IV in 137 samples. The patient's clinical details are summarized in Table 2.

For qRT–PCR, 137 ccRCC samples and 77 corresponding normal adjacent samples were used. Samples were FFPE tissues from 137 patients who had undergone surgical excision for ccRCC.

MiRNA extraction and qRT–PCR

MiRNA was extracted using a RecoverAll Total Nucleic Acid Isolation Kit for FFPE tissues (Ambion, Foster City, CA, USA). Reverse transcription was carried out using a TaqMan microRNA reverse transcription kit (Applied Biosystems, Foster City, CA, USA) according to the manufacturer's protocol. Hsa-miR-155 was detected using TaqMan MicroRNA assays (Assay ID 000479; Applied Biosystems). Real-time quantification of cDNA was carried out on a 7900HT Fast Real-Time PCR System (Applied Biosystems). Expression data were normalized according to expression of the RNU48 reference DNA (Assay ID 001006; Applied Biosystems).[22]

Immunohistochemistry

IHC was carried out on 4-μm thick sections of FFPE. Immunohistochemical analysis was carried out with a Dako EnVision+ System- HRP Labelled Polymer anti-mouse (Dako Cytomation, Carpinteria, CA, USA). Antigen retrieval for HIF-1α was carried out by microwave heating in citrate buffer (pH 6.0) for 30 min. After peroxidase activity had been blocked with 1% H_2O_2 / 50% methanol for 10 min, HIF-1α was detected with a mouse monoclonal antibody Mab H1α67 (1:200; Novus Biologicals, Littleton, CO, USA). A total of 64 sections were incubated with primary antibody for 1 h at room temperature, and then with Dako EnVision+ System- HRP Labelled Polymer anti-mouse for 1 h. For color reaction, sections were incubated with 3,3′-diaminobenzidine Substrate-Chromogen Solution (Dako Cytomation) for 3 s. Sections were counterstained with 0.1% hematoxylin. The cut-off point for antibody reactivity necessary to define a result as positive was staining of any cells with nuclear localization in surgically resected specimens.

IHC was carried out on 64 ccRCC samples, including 39 with the lowest expression of miR-155 tissue and 25 with the highest expression of miR-155 tissues of 137 patients who had undergone surgical excision for ccRCC.

Statistical analysis

Statistical differences between miRNA expression levels in ccRCC samples and normal kidney samples were evaluated using the Wilcoxon matched pairs test. Statistical differences of RNU48 reference DNA were evaluated using the non-parametric Mann–Whitney *U*-test. For analysis of correlation between expression levels of miR-155 and tumor size, we used the non-parametric Spearman's rank correlation coefficient. The correlation between expression levels

Table 1 Clinical characteristics of the 137 ccRCC patients

			Expression of miR-155		*P*-value
			Low	High	
Sex (%)		Sex (%)			0.0426
Male	103 (75)	Male	103 (75)	46	57
Female	34 (25)	Female	34 (25)	22	12
Side (%)		Side (%)			NS
Left	59 (43)	Left	59 (43)	24	35
Right	78 (57)	Right	78 (57)	44	34
Median age, years (range)		Median age, years (%)			NS
	66 (34–89)	<65	64 (47)	34	30
		≥65	73 (53)	34	39
Histological grade (%)		Histological grade (%)			NS
G1	60 (44)	G1–2	103 (75)	56	47
G2	43 (31)	G3–4	34 (25)	12	22
G3	31 (23)				
G4	3 (2)				
Infiltrating type (%)		Infiltrating type (%)			NS
INFa	113 (82)	INFa	113 (82)	57	56
INFb	23 (17)	INFb/c	24 (18)	11	13
INFc	1 (1)				
pT stage (%)		pT stage (%)			NS
pT1	83 (61)	pT1–2	99 (72)	52	47
pT2	16 (12)	pT3–4	38 (28)	16	22
pT3	36 (26)				
pT4	2 (1)				
pN stage (%)		pN stage (%)			NS
pNx	79 (58)	pNx/0	129 (94)	66	63
pN0	50 (36)	pN1/2	8 (6)	2	6
pN1/2	8 (6)				
Venous invasion (%)		Venous invasion (%)			NS
v0	93 (68)	v0	93 (68)	49	44
v1	44 (32)	v1	44 (32)	19	25
M stage (%)		M stage (%)			NS
M0	117 (85)	M0	117 (85)	60	57
M1	20 (15)	M1	20 (15)	8	12
Stage grouping (%)		Stage grouping			NS
Stage I	81 (59)	Stage I/II	94 (68)	50	44
Stage II	13 (9)	Stage III/IV	43 (32)	18	25
Stage III	23 (17)				
Stage IV	20 (15)				
Observation period (months)					
Median	65				
Range	2–188				

The expression levels of miR-155 were divided into two groups, low and high expression of miR-155, based on the median miR-155 expression level (cut-off line = the median miR-155 expression level in this group). Corresponding median value = –0.0831.

of miR-155, clinicopathological parameters and expression of HIF-1α in IHC was analyzed with Fisher's exact test. A log–rank test and Kaplan–Meier plots were constructed for the miR-155-high and miR-155-low groups. Univariate and multivariate analysis of factors influencing survival were carried out using the Cox proportional hazards model. And parameters at multivariate analysis were selected by the stepwise method. The HR and 95% CI were estimated from

Table 2 Clinical characteristics of 43 stage III and IV ccRCC patients

				Expression of miR-155		*P*-value
				Low	High	
Sex (%)		Sex (%)				NS
Male	39 (90)	Male	39 (90)	18	21	
Female	4 (10)	Female	4 (10)	3	1	
Side (%)		Side (%)				NS
Left	14 (33)	Left	14 (33)	6	8	
Right	29 (67)	Right	29 (67)	15	14	
Median age, years (range)		Median age, years (%)				NS
	66 (45–89)	<65	21 (49)	10	11	
		≥65	22 (51)	11	11	
Histological grade (%)		Histological grade (%)				NS
G1	7 (16)	G1–2	22 (59)	11	11	
G2	15 (35)	G3–4	21 (51)	11	10	
G3	18 (42)					
G4	3 (7)					
Infiltrating type (%)		Infiltrating type (%)				NS
INFa	25 (58)	INFa	25 (58)	13	12	
INFb	17 (40)	INFb/c	18 (42)	8	10	
INFc	1 (3)					
pT stage (%)		pT stage (%)				NS
pT1	2 (5)	pT1–2	5 (12)	3	2	
pT2	3 (7)	pT3–4	38 (88)	18	20	
pT3	36 (84)					
pT4	2 (5)					
pN stage (%)		pN stage (%)				NS
pNx	7 (16)	pNx/0	35 (81)	17	18	
pN0	28 (65)	pN1/2	8 (19)	4	4	
pN1/2	8 (19)					
Venous invasion (%)		Venous invasion (%)				NS
v0	8 (19)	v0	8 (19)	5	3	
v1	35 (81)	v1	35 (81)	16	19	
M stage (%)		M stage (%)				NS
M0	23 (53)	M0	23 (53)	10	13	
M1	20 (47)	M1	20 (47)	11	9	
Observation period (months)						
Median	43					
Range	2–188					

The expression levels of miR-155 were divided into two groups, low and high expression of miR-155, based on the median miR-155 expression level (cut-off line = the median miR-155 expression level in this group). Corresponding median value = −0.0811.

the Cox proportional hazard model. Wilcoxon matched pairs test, Pearson's product-moment correlation coefficient, Fisher's exact test, a log–rank test and Kaplan–Meier plots were calculated using JMP software version 10 (SAS Institute, Cary, NC, USA). The Cox proportional hazards model, stepwise method and concordance, R^2 and Wald test were calculated using the R statistical environment (http://www.R-project.org). For all analyses, age was treated as a categorical variable (65 years or more *vs* less than 65 years). A *P*-value of less than 0.05 was considered statistically significant.

Results

Expression levels of miR-155 between ccRCC and normal kidney tissues

We analyzed 77 matched pairs of ccRCC and normal adjacent kidney tissues from the same patients by qRT–PCR. To

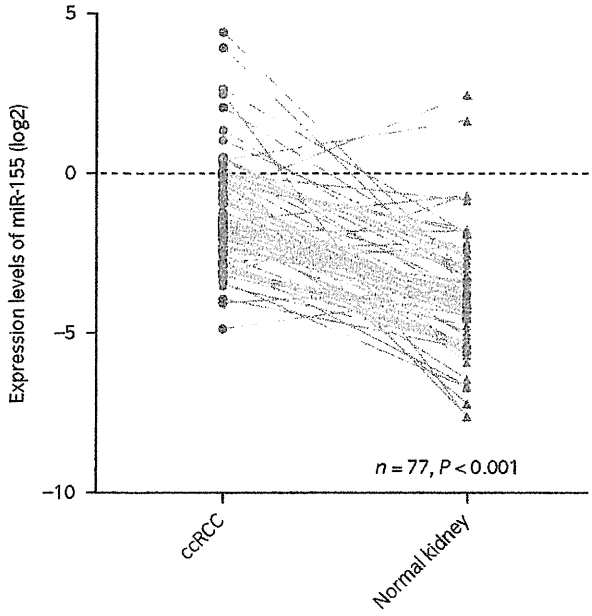

Fig. 1 Expression of miR-155 between tumor and normal kidney tissue in 77 ccRCC samples in all stages ($P < 0.001$).

show the usefulness of RNU48 as a reference gene, we analyzed the expression of RNU48 between tumors and normal adjacent kidney tissue in 77 matched pairs of ccRCC samples (Fig. S1a). The expression level of RNU48 in some clinicopathological parameters in 137 ccRCC samples was also examined (Fig. S1b). The expression level of RNU48 showed no significant difference between tumors and normal adjacent kidney, and also among all clinicopathological parameters. Therefore, we confirmed that RNU48 is stably expressed in ccRCC and is useful as a reference gene.

Differences between the two groups were evaluated using the Wilcoxon matched pairs test. Highly significant differences were identified between 77 ccRCC with all stages and normal adjacent kidney tissues in the expression levels of miR-155 ($P < 0.001$), as well as limited to 63 ccRCC with stage I and II ($P < 0.001$), and 14 ccRCC with stage III and IV ($P = 0.0138$; Fig. 1).

Relationship between miR-155 expression and tumor size

We analyzed the correlation between expression levels of miR-155 and tumor size in 123 ccRCC tissues in which the tumor sizes had been established. Tumor size ranged between 0.8 and 17 cm, with a median of 4.6 cm. For analysis of the correlation between expression levels of miR-155 and tumor size, we used the non-parametric Spearman's rank correlation coefficient. There were no statistically significant differences, but expression levels of miR-155 tended to be associated with a tumor size ($r = 0.2045$, $P = 0.0943$; Fig. 2).

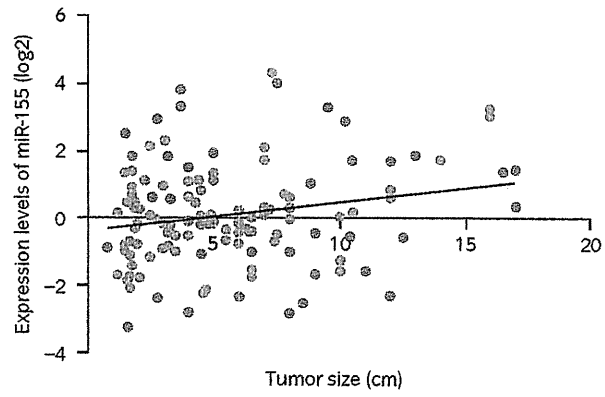

Fig. 2 Correlation between expression levels of miR-155 and tumor size in 123 samples. Pearson's product-moment correlation coefficient 0.2045 ($P = 0.0943$).

Expression levels of miR-155 and clinical prognosis

To determine the difference in CSS and CFS on the basis of expression levels of miR-155, we divided the sample into two groups (low and high expression levels of miR-155) based on the median miR-155 expression level in the group. Kaplan–Meier plots were constructed in 137 ccRCC with all stages. This analysis showed no association with prognosis ($P = 0.7001$; Fig. 3a). In contrast, when limited to the stage III and IV groups, the analysis showed significant differences for CSS on the basis of miR-155 expression levels; low expression levels of miR-155 were correlated with poor prognosis in Kaplan–Meier plots and log–rank tests ($P = 0.0337$; Fig. 3b). Regarding the CFS of 26 patients with stage III and IV ccRCC who had received curative resection, means status of no visible residual tumor clinically after radical nephrectomy with or without metastatectomy. Low expression levels of miR-155 tended to be associated with a high rate of recurrence ($P = 0.0614$; Fig. 3c). We also analyzed CSS in 31 patients who had received postoperative IFN-α therapy after radical nephrectomy, and found that low expression levels of miR-155 were associated with poor prognosis ($P = 0.0464$; Fig. 3d).

Univariate and multivariate analysis of factors influencing survival

In univariate analyses, M stage, histological grade, infiltrating type, pT stage and pN stage were correlated with poor prognosis. Although high expression levels of miR-155 in univariate analysis were not correlated with poor prognosis, the independent predictors in the multivariate analysis were M stage, pT stage, pN stage and low expression levels of miR-155 (Table 3). In univariate analysis confined to patients with stage III and IV ccRCC, M stage, pN stage and low expression levels of miR-155 were correlated with poor

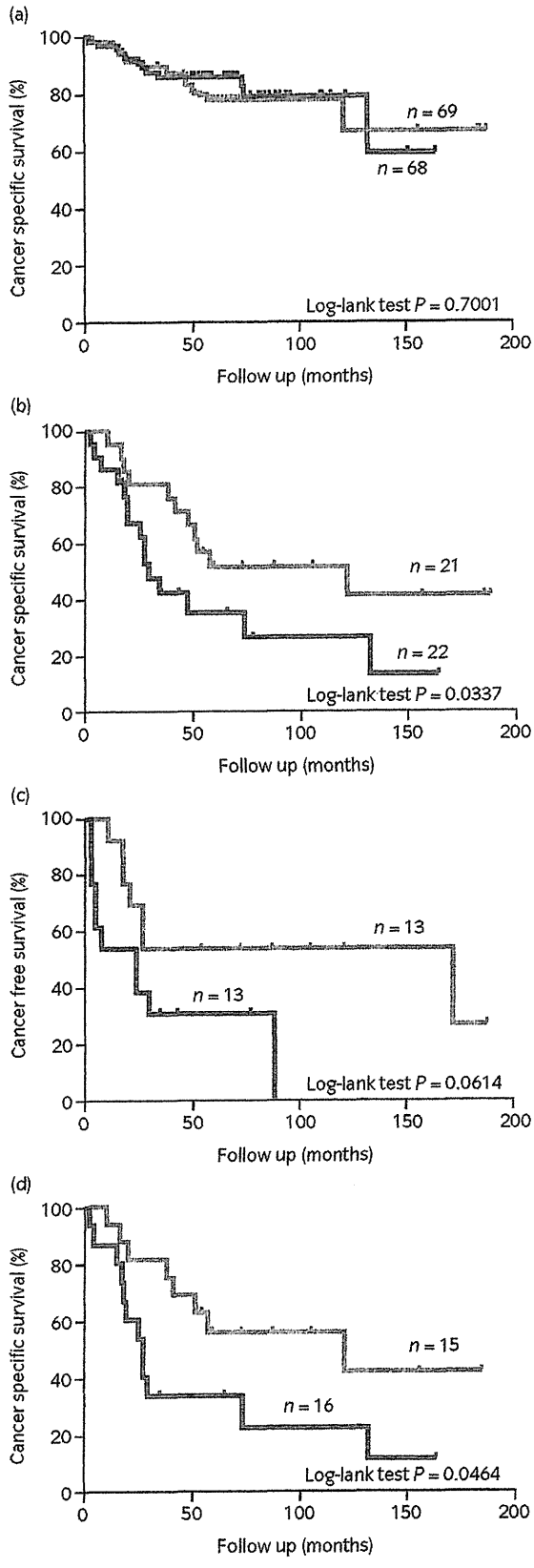

Fig. 3 (a) CSS of 137 patients with ccRCC based on the expression levels of miR-155 (cut-off line = the median miR-155 expression level in this group). Corresponding median value = –0.0831; $P = 0.7001$. (b) CSS of 43 patients with ccRCC based on the expression levels of miR-155 (cut-off line = the median miR-155 expression level in this group) in stage III and IV. Corresponding median value = –0.0811; $P = 0.0337$. (c) CFS of 26 patients after undergoing curative resection for ccRCC based on the expression levels of miR-155 (cut-off line = the median miR-155 expression level in this group) in stage III and IV. Corresponding median value = 0.6190; $P = 0.0614$. (d) CSS of 31 patients with ccRCC based on expression levels of miR-155 (cut-off line = the median miR-155 expression level in this group) in 31 patients who received postoperative therapy with IFN-α after radical nephrectomy. Corresponding median value = 0.59781; $P = 0.0464$. ——, miR-155 high; ——, miR-155 low.

prognosis. Independent predictors in multivariate analysis were M stage, histological grade, pT stage and low expression levels of miR-155. These experiments yielded that low expression of miR-155 was an independent indicator of poor prognosis (Table 4).

Relationship between HIF-1α expression and expression of miR-155

We used IHC to investigate the association between HIF-1α expression and expression of miR-155 in 64 ccRCC samples that included 39 lowest expression of miR-155 tissue and 25 highest expression of miR-155 tissues in the 137 samples we analyzed.

In the 39 low expression levels of miR-155 ccRCC, the HIF-1α positive and HIF-1α negative tumor frequency were 17 out of 39 (44%) and 22 out of 39 (56%). In contrast, in the 25 high expression of miR-155 ccRCC, the HIF-1α positive and HIF-1α negative tumor frequency were 17 out of 25 (66%) and eight out of 25 (32%; Fig. 4). For analysis of the correlation between expression of miR-155 and HIF-1α, we used the Fisher's exact test. This difference was not statically significant, but high expression levels of miR-155 tended to be associated with a high HIF-1α expression ($P = 0.0744$; Table 5).

Discussion

RCC remains to be one of the leading causes of death, so finding new molecular targets for its diagnosis, prognosis and treatment has the potential to improve the clinical strategies and outcomes of this disease. One of the most frequently studied miRNA in cancer biology, miR-155, has also been repeatedly identified through miRNA microarray profiling as upregulated in ccRCC tissue. It has been

Table 3 Univariate and multivariate analysis of factors influencing survival in 137 patients with ccRCC

	Univariate analysis			Multivariate analysis			
	Hazard ratio	95% CI	*P*-value	Hazard ratio	95% CI	Robust SE	*P*-value
Sex							
Female	1		0.0539	Non-selected			
Male	4.12	0.98–17.42					
Age (years)							
<65	1		0.411	Non-selected			
≥65	1.01	0.98–1.05					
Side							
Right	1		0.9930	1		0.612	0.1500
Left	1.01	0.46–2.17		2.44	0.73–8.10		
M stage							
cM0	1		<0.0001	1		0.485	<0.0001
cM1	18.31	8.18–41.02		8.6	3.33–22.25		
Histological grade							
G1/2	1		<0.0001	1		0.608	0.0710
G3/4	5.30	2.46–11.42		3.00	0.91–9.99		
INF							
INF a	1		<0.0001	Non-selected			
INF b/c	6.51	3.02–14.08					
pT							
pT1/2	1		<0.0001	1		0.959	0.0055
pT3/4	19.73	6.77–57.52		14.37	2.19–94.17		
pN stage							
pNx/0	1		<0.0001	1		0.461	0.0380
pN1/2	10.68	4.33–26.38		2.60	1.05–6.42		
Expression of miR-155							
High (>median)	1		0.9850	1		0.421	0.0001
Low (≤median)	0.99	0.47–2.11		5.49	2.40–12.52		

Concordance = 0.946 (SE = 0.059), R^2 = 0.493, Wald test = 52.93 on 6 d.f. (P < 0.0001).

reported that miR-155 levels are almost 30-fold higher in ccRCC compared with normal tissues.[16] Consistent with this result, our qRT–PCR analysis showed that expression levels of miR-155 were 6.2-fold higher in 77 matched pairs of ccRCC than in normal adjacent kidney tissues (P < 0.001). The correlation between high expression levels of miR-155 and tumor size in ccRCC has been reported,[7,8] and we also confirmed a significant association between expression of miR-155 and tumor size (r = 0.2045, P = 0.0238). The available experimental evidence indicates that miR-155 is overexpressed in a variety of malignant tumors. MiR-155 behaves as an oncogenic miRNA in breast cancer, lung cancer, hepatocellular carcinoma, colorectal cancer and pancreatic tumors.[17–21] It has been reported that miR-155 downregulates many tumor suppressor genes that repress PI3K or apoptosis-related signaling.[17,23,24] MiR-155 can be attributed to ccRCC tumor progression.

A significant correlation was found between low expression levels of miR-155 and prognosis in 43 patients with stage III and IV ccRCC using the log–rank test, and univariate and multivariate analysis. Especially in multivariate analysis, low expression levels of miR-155 showed a strong correlation with poor prognosis (P = 0.0010), and the CFS of 26 patients who had received curative resection tended to be associated with low expression levels of miR-155. We also found a significant correlation between low expression levels of miR-155 and prognosis in 31 patients who had received postoperative therapy with IFN-α after radical nephrectomy. These results are inconsistent with the results of all 137 cases. In general, the central part of a tumor will be in an ischemic and hypoxic state. Tumor cells undergo a variety of biological responses when placed in hypoxic conditions, including activation of signaling pathways that regulate proliferation, angiogenesis and cell death by the transcription factor HIF-1α.[25] The overexpression of HIF-1α is one of the important characteristic genetic abnormalities in ccRCC.[26] It has also been reported that hypoxia-induced miR-155 plays a role as a component of a network of negative feedback loops that controls HIF-1α translation.[27] It is well known that HIF-1α overexpression is a